UPPSALA
UNIVERSITET

Nonlinear Identification of Individualized Drug Effect Models of the Neuromuscular Blockade in Anesthesia

Alexander Medvedev

September 22, 2015

alexander.medvedev@it.uu.se

Co-authors

- Olov Rosén, Öhlins – Advanced Suspension Technology, Sweden
- Margarida M. Silva, Bosch, Vienne, Austria
- Zhanybai T. Zhusubaliyev, South-West State University, Kursk, Russia

alexander.medvedev@it.uu.se

Outline

This talk is a nutshell

1. A method to control slowly varying Wiener systems by PID without oscillations

alexander.medvedev@it.uu.se

UPPSALA UNIVERSITET

This talk is a nutshell

1. A method to control slowly varying Wiener systems by PID without oscillations
2. Particle filter is the best way of estimating Wiener models of drug administration.

alexander.medvedev@it.uu.se

Closed-loop drug delivery

Automatic dosing of the drug by a feedback controller from quantified symptoms:

- Individualization of treatment

alexander.medvedev@it.uu.se

UPPSALA UNIVERSITET

Closed-loop drug delivery

Automatic dosing of the drug by a feedback controller from quantified symptoms:

- Individualization of treatment
- Intrinsic monitoring of the patient state

alexander.medvedev@it.uu.se

Closed-loop drug delivery

Automatic dosing of the drug by a feedback controller from quantified symptoms:

- Individualization of treatment
- Intrinsic monitoring of the patient state
- Automation of tedious dose adjustment

alexander.medvedev@it.uu.se

Closed-loop drug delivery

Automatic dosing of the drug by a feedback controller from quantified symptoms:

- Individualization of treatment
- Intrinsic monitoring of the patient state
- Automation of tedious dose adjustment
- Suitable for remote operation

alexander.medvedev@it.uu.se

Closed-loop drug delivery

Automatic dosing of the drug by a feedback controller from quantified symptoms:

- Individualization of treatment
- Intrinsic monitoring of the patient state
- Automation of tedious dose adjustment
- Suitable for remote operation

Prerequisites:

- Sensor (monitor) quantifying the symptoms

alexander.medvedev@it.uu.se

Closed-loop drug delivery

Automatic dosing of the drug by a feedback controller from quantified symptoms:

- Individualization of treatment
- Intrinsic monitoring of the patient state
- Automation of tedious dose adjustment
- Suitable for remote operation

Prerequisites:

- Sensor (monitor) quantifying the symptoms
- Controller guaranteeing that the symptoms closely follow the set point prescribed by medical personnel

alexander.medvedev@it.uu.se

Closed-loop drug delivery

Automatic dosing of the drug by a feedback controller from quantified symptoms:

- Individualization of treatment
- Intrinsic monitoring of the patient state
- Automation of tedious dose adjustment
- Suitable for remote operation

Prerequisites:

- Sensor (monitor) quantifying the symptoms
- Controller guaranteeing that the symptoms closely follow the set point prescribed by medical personnel
- Drug dosing device (pump, dispenser, vaporizer, etc.)

Anesthesia: Neuromuscular Blockade (NMB)

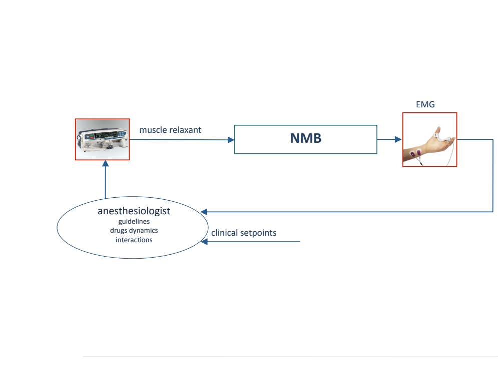

NMB – neuromuscular blockade; EMG – blockade level measured by electromyogram; muscle relaxant — atracurium; reactive and predictive control of blockade level by anaesthesiologist

alexander.medvedev@it.uu.se

Anesthesia: KMG NMB sensor

KMG NMB sensor: The electrical stimulation of the adductor pollicis muscle is performed via the two electrodes on the wrist of the patient and the response is measured by the motion of the thumb. Unrelated with the NMB measurement, there is a finger oximeter placed on the middle finger of the patient.

alexander.medvedev@it.uu.se

Closed-loop Anesthesia: PID

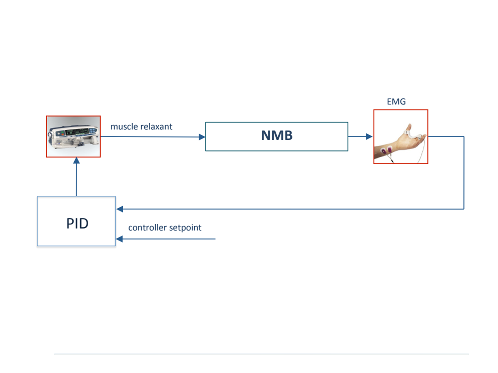

NMB – neuromuscular blockade; EMG – blockade level measured by electromyogram; muscle relaxant — atracurium; PID – proportional, intergal and derivative controller

alexander.medvedev@it.uu.se

Closed-loop drug delivery

Challenges

- Difficulties in translating control performance into clinical outcome

alexander.medvedev@it.uu.se

Closed-loop drug delivery

Challenges

- Difficulties in translating control performance into clinical outcome
- High inter-patient and intra-patient variability

alexander.medvedev@it.uu.se

Closed-loop drug delivery

Challenges

- Difficulties in translating control performance into clinical outcome
- High inter-patient and intra-patient variability
  - High inter-patient variability: individualized controller

alexander.medvedev@it.uu.se

Closed-loop drug delivery

Challenges

- Difficulties in translating control performance into clinical outcome
- High inter-patient and intra-patient variability
  - High inter-patient variability: individualized controller
  - High intra-patient variability: adaptivity

alexander.medvedev@it.uu.se

Closed-loop drug delivery

Challenges

- Difficulties in translating control performance into clinical outcome
- High inter-patient and intra-patient variability
  - High inter-patient variability: individualized controller
  - High intra-patient variability: adaptivity
- Implementation of predictive action

alexander.medvedev@it.uu.se

UPPSALA UNIVERSITET

Closed-loop drug delivery

Challenges

- Difficulties in translating control performance into clinical outcome
- High inter-patient and intra-patient variability
  - High inter-patient variability: individualized controller
  - High intra-patient variability: adaptivity
- Implementation of predictive action
- Oscillations: interchanging underdosing and overdosing episodes

alexander.medvedev@it.uu.se

Closed-loop drug delivery

Challenges

- Difficulties in translating control performance into clinical outcome
- High inter-patient and intra-patient variability
  - High inter-patient variability: individualized controller
  - High intra-patient variability: adaptivity
- Implementation of predictive action
- Oscillations: interchanging underdosing and overdosing episodes
  - Underdosing: insufficient drug effect

alexander.medvedev@it.uu.se

Closed-loop drug delivery

Challenges

- Difficulties in translating control performance into clinical outcome
- High inter-patient and intra-patient variability
  - High inter-patient variability: individualized controller
  - High intra-patient variability: adaptivity
- Implementation of predictive action
- Oscillations: interchanging underdosing and overdosing episodes
  - Underdosing: insufficient drug effect
  - Overdosing: risk of side effects

alexander.medvedev@it.uu.se

UPPSALA UNIVERSITET

Closed-loop drug delivery

Challenges

- Difficulties in translating control performance into clinical outcome
- High inter-patient and intra-patient variability
  - High inter-patient variability: individualized controller
  - High intra-patient variability: adaptivity
- Implementation of predictive action
- Oscillations: interchanging underdosing and overdosing episodes
  - Underdosing: insufficient drug effect
  - Overdosing: risk of side effects
  - Oscillation: both of the above

alexander.medvedev@it.uu.se

Closed-loop drug delivery: PID-control of BIS

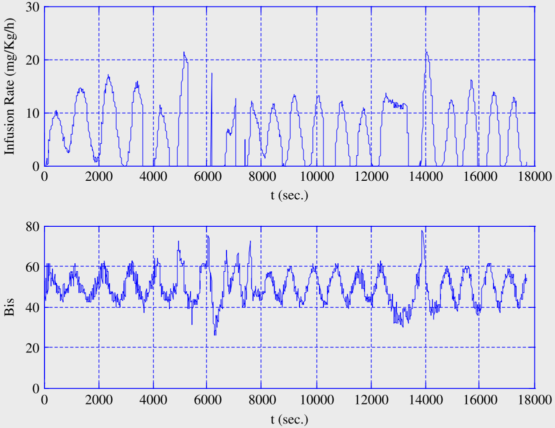

Oscillations in PID-controlled anesthesia. Appropriate BIS level for general anesthesia is from 40 to 60. From Méndez et al, Computer Methods in Biomechanics and Biomedical Engineering Vol. 12, No. 6, December 2009, pp. 727–734

alexander.medvedev@it.uu.se

Closed-loop drug delivery

Avoiding oscillations

- How far is the closed loop from oscillation?

alexander.medvedev@it.uu.se

Closed-loop drug delivery

Avoiding oscillations

- How far is the closed loop from oscillation?
- How to design a controller that is farther from oscillation?

alexander.medvedev@it.uu.se

UPPSALA UNIVERSITET

Closed-loop drug delivery

Avoiding oscillations

- How far is the closed loop from oscillation?
- How to design a controller that is farther from oscillation?
- If there is a risk for oscillations, how to safely move the closed-loop system to better controller settings?

alexander.medvedev@it.uu.se

Closed-loop drug delivery

Avoiding oscillations

- How far is the closed loop from oscillation?
- How to design a controller that is farther from oscillation?
- If there is a risk for oscillations, how to safely move the closed-loop system to better controller settings?

alexander.medvedev@it.uu.se

Closed-loop drug delivery

Avoiding oscillations

- How far is the closed loop from oscillation?
- How to design a controller that is farther from oscillation?
- If there is a risk for oscillations, how to safely move the closed-loop system to better controller settings?

Zh. Zhusubaliyev, A. Medvedev, and M. Silva "Bifurcation Analysis of PID Controlled Neuromuscular Blockade in Closed-loop Anesthesia", Journal of Process Control, Volume 25, January 2015, Pages 152–163.

Zh. Zhusubaliyev, M. Silva, and A. Medvedev "Automatic recovery from nonlinear oscillations in PID-controlled anesthetic drug delivery", European Control Conference, Linz, Austria, July, 2015

alexander.medvedev@it.uu.se

Closed-loop drug delivery

Avoiding oscillations

- How far is the closed loop from oscillation?
- How to design a controller that is farther from oscillation?
- If there is a risk for oscillations, how to safely move the closed-loop system to better controller settings?

Zh. Zhusubaliyev, A. Medvedev, and M. Silva "Bifurcation Analysis of PID Controlled Neuromuscular Blockade in Closed-loop Anesthesia", Journal of Process Control, Volume 25, January 2015, Pages 152–163.

Zh. Zhusubaliyev, M. Silva, and A. Medvedev "Automatic recovery from nonlinear oscillations in PID-controlled anesthetic drug delivery", European Control Conference, Linz, Austria, July, 2015

Accurate pharmacodynamic-pharmacokinetic models are necessary.

alexander.medvedev@it.uu.se

Mathematical modeling: The patient model

The system (PK/PD) is modeled by a Wiener model:

- The linear block is of third order, with the parameter α

$$\dot{x}_1 = -\alpha k_3(x_1 - u(t)), \quad \dot{x}_2 = \alpha k_2(x_1 - x_2),$$
$$\dot{x}_3 = \alpha k_1(x_2 - x_3),$$

- The nonlinearity is a Hill function of order $\gamma \in \mathbb{R}^+$

$$y(t) = \frac{100\, C_{50}^{\gamma}}{C_{50}^{\gamma} + x_3^{\gamma}(t)}.$$

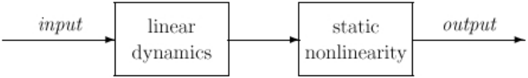

- The patient model is parameterized in two parameters α, γ.

alexander.medvedev@it.uu.se

Mathematical modeling: PID controller

PID controller with time-varying gain

$$u(t) = K(t)\left(e(t) + \frac{1}{T_i}\int e(s)\; ds + T_d\,\frac{de(t)}{dt}\right),$$

with

$$\dot{K}(t) = -\xi\,(K(t) - K_*)\,.$$

- $e(t) = y_{\mathsf{r}} - y(t)$ is the control error
- y_{r} is the reference to be followed.

alexander.medvedev@it.uu.se

Mathematical modeling: closed-loop

The mathematical model of the closed-loop NMB

$$\frac{d\mathbf{x}}{dt} = \mathbf{f}(\mathbf{x}), \tag{1}$$

$$\mathbf{x} = (x_1, x_2, x_3, x_4, x_5)^T,$$

$$\mathbf{f}(\mathbf{x}) = (f_1, f_2, f_3, f_4, f_5)^T,$$

with

$$\begin{aligned} f_1 &= -\alpha\, k_3\, x_1 - \alpha^2\, k_1\, k_3\, T_d\; x_5 \Phi'(x_3)(x_2 - x_3) \\ &\quad + \alpha\, k_3\, x_5 (y_{\mathsf{r}} - \Phi(x_3)) + \frac{\alpha k_3}{T_i} x_4\, x_5, \\ f_2 &= \alpha\, k_2 (x_1 - x_2), \quad f_3 = \alpha k_1 (x_2 - x_3), \\ f_4 &= y_{\mathsf{r}} - \Phi(x_3), \quad f_5 = -\xi\,(x_5 - K_*), \\ \Phi'(x_3) &= -\frac{\gamma x_3^{\gamma-1}}{100\, C_{50}^{\gamma}}\, \Phi^2(x_3). \end{aligned}$$

alexander.medvedev@it.uu.se

Analysis: equilibrium state

The closed-loop system has a single equilibrium state $\mathbf{x}_* = [x_1^*, x_2^*, x_3^*, x_4^*, x_5^*]^T$, where

$$x_1^* = x_2^* = x_3^*, \quad x_4^* = \frac{T_i}{K_*} x_3^*,$$

$$x_3^* = C_{50} \left(\frac{100}{y_\mathrm{r}} - 1 \right)^{\frac{1}{\gamma}}, x_5^* = K_*.$$

The local stability of $\mathbf{x}_*$ is determined by the eigenvalues of

$$\mathbf{Df}(\mathbf{x}_*) = \left[\frac{\partial f_i}{\partial x_j} \right]_{1 \leqslant i \leqslant 5;\, 1 \leqslant j \leqslant 5},$$

- Real part: the rate of growth in response to perturbation away from the equilibrium point
- Imaginary part: the angular frequency of an oscillatory component of the dynamics

alexander.medvedev@it.uu.se

Analysis: distance to bifurcation

Andronov-Hopf bifurcation

The transition in which a pair of complex conjugated eigenvalues simultaneously crosses the imaginary axis from the left to the right complex half-plane.

Analysis: distance to bifurcation

Andronov-Hopf bifurcation

The transition in which a pair of complex conjugated eigenvalues simultaneously crosses the imaginary axis from the left to the right complex half-plane.

The surface in the parameter space $(T_d, T_i, K_*, \alpha, \gamma)$

$$\chi(T_i, T_d, K_*, \alpha, \gamma) = b_3^2 - b_1 b_2 b_3 + b_1^2 b_4 = 0 \tag{2}$$

defines the stability boundary of the equilibrium.

$$\begin{aligned}
b_1 &= \alpha(k_1 + k_2 + k_3), \\
b_2 &= \alpha^2\,(k_1\,k_2 + k_1\,k_3 + k_2\,k_3) \\
&\quad + \alpha^3\,k_1\,k_2\,k_3\,K_*\,T_d\,\Phi'(x_3^*), \\
b_3 &= \alpha^3\,k_1\,k_2\,k_3\left[1 + K_*\Phi'(x_3^*)\right], \\
b_4 &= \frac{\alpha^3\,k_1\,k_2\,k_3\,K_*}{T_i}\Phi'(x_3^*).
\end{aligned} \tag{3}$$

Analysis: distance to bifurcation

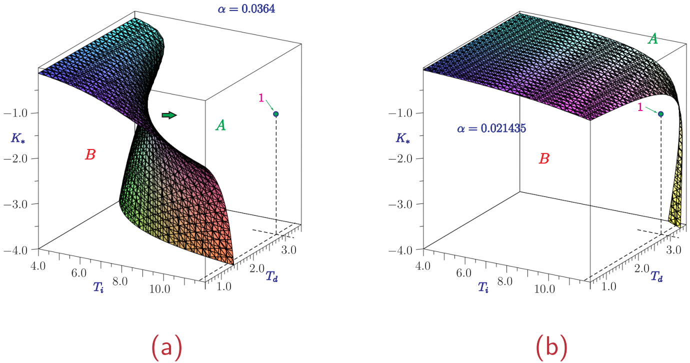

Figure: (a) Andronov-Hopf bifurcation boundary in the parameter space (T_i, T_d, K_*) for $\alpha = 0.0364$ and $\gamma = 4.24358$: A is the equilibrium stability domain, B is the region of unstable equilibrium. Point 1 belongs to A. (b) Andronov-Hopf bifurcation boundary in the parameter space (T_i, T_d, K_*) for $\alpha = 0.021435$ and $\gamma = 4.24358$. Now Point 1 is in B.

 alexander.medvedev@it.uu.se

Analysis: distance to bifurcation

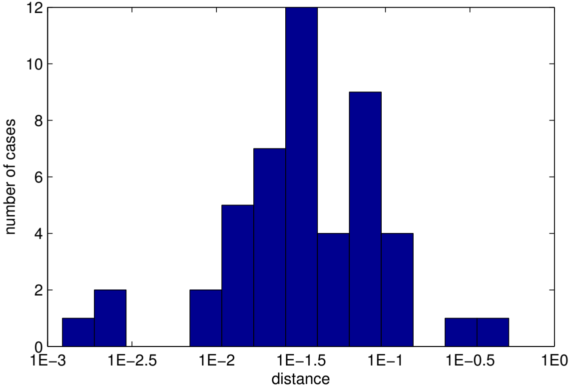

Figure: Histogram of the distance to bifurcation, at time $t = 40$ min, over the 48 cases in the synthetic database, assuming PID control. Note the log-scale on the x-axis. Three cases are at high risk of oscillations

alexander.medvedev@it.uu.se

Analysis: the impact of $K(t)$

The eigenvalues of the Jacobian matrix are determined by

$$\begin{aligned}&\det\left(\mathbf{Df}(\mathbf{x}_*) - s\mathbf{I}\right) = \\ &= (s^4 + b_1 s^3 + b_2 s^2 + b_3 s + b_4)(s+\xi) = 0.\end{aligned}$$

The factor $(s+\xi)$ is independent of the system parameters.

alexander.medvedev@it.uu.se

Analysis: the impact of $K(t)$

The eigenvalues of the Jacobian matrix are determined by

$$\det\left(\mathbf{Df}(\mathbf{x}_*) - s\mathbf{I}\right) =$$
$$= (s^4 + b_1 s^3 + b_2 s^2 + b_3 s + b_4)(s + \xi) = 0.$$

The factor $(s + \xi)$ is independent of the system parameters.

No new nonlinear dynamical behaviors arise due to the time-varying PID controller.

The surgery room scenario

- A Wiener individualized NMB model is estimated from a drug bolus response.

alexander.medvedev@it.uu.se

The surgery room scenario

- A Wiener individualized NMB model is estimated from a drug bolus response.
- From the desired controller convergence rate and distance to bifurcation, the gains of the PID controller K_0, T_i, T_d are calculated, see [JPC2015].

alexander.medvedev@it.uu.se

UPPSALA UNIVERSITET

The surgery room scenario

- A Wiener individualized NMB model is estimated from a drug bolus response.
- From the desired controller convergence rate and distance to bifurcation, the gains of the PID controller K_0, T_i, T_d are calculated, see [JPC2015].
- The parameters α, γ and the distance to bifurcation are estimated on-line while the surgery proceeds.

alexander.medvedev@it.uu.se

The surgery room scenario

- A Wiener individualized NMB model is estimated from a drug bolus response.
- From the desired controller convergence rate and distance to bifurcation, the gains of the PID controller K_0, T_i, T_d are calculated, see [JPC2015].
- The parameters α, γ and the distance to bifurcation are estimated on-line while the surgery proceeds.
- When the estimated distance to bifurcation goes under a given threshold, of the PID controller is re-designed giving K_{ref}.

The surgery room scenario

- A Wiener individualized NMB model is estimated from a drug bolus response.
- From the desired controller convergence rate and distance to bifurcation, the gains of the PID controller K_0, T_i, T_d are calculated, see [JPC2015].
- The parameters α, γ and the distance to bifurcation are estimated on-line while the surgery proceeds.
- When the estimated distance to bifurcation goes under a given threshold, of the PID controller is re-designed giving K_{ref}.
- The recovery controller is activated for $K_0 \to K_{ref}$.

alexander.medvedev@it.uu.se

The surgery room scenario

- A Wiener individualized NMB model is estimated from a drug bolus response.
- From the desired controller convergence rate and distance to bifurcation, the gains of the PID controller K_0, T_i, T_d are calculated, see [JPC2015].
- The parameters α, γ and the distance to bifurcation are estimated on-line while the surgery proceeds.
- When the estimated distance to bifurcation goes under a given threshold, of the PID controller is re-designed giving K_{ref}.
- The recovery controller is activated for $K_0 \to K_{ref}$.

alexander.medvedev@it.uu.se

The surgery room scenario

- A Wiener individualized NMB model is estimated from a drug bolus response.
- From the desired controller convergence rate and distance to bifurcation, the gains of the PID controller K_0, T_i, T_d are calculated, see [JPC2015].
- The parameters α, γ and the distance to bifurcation are estimated on-line while the surgery proceeds.
- When the estimated distance to bifurcation goes under a given threshold, of the PID controller is re-designed giving K_{ref}.
- The recovery controller is activated for $K_0 \rightarrow K_{ref}$.

Zhusubaliyev, Medvedev, Silva, Bifurcation analysis of PID-controlled neuromuscular blockade in closed-loop anesthesia, *Journal of Process Control* v. 25, January 2015, pp. 152-163

alexander.medvedev@it.uu.se

Simulation experiment: parameter changes

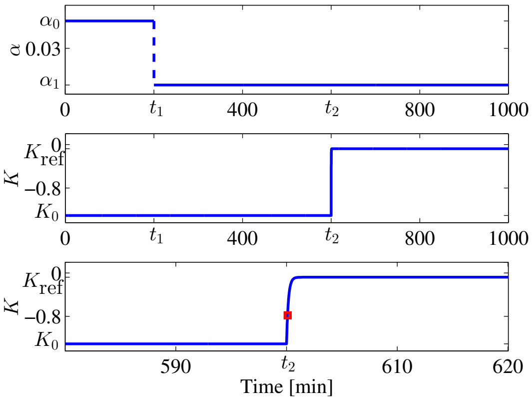

Figure: Time-domain changes in α and K, for $\xi = 0.1$. The red square depicts the value of K_{bif}.

alexander.medvedev@it.uu.se

Simulation experiment: system output

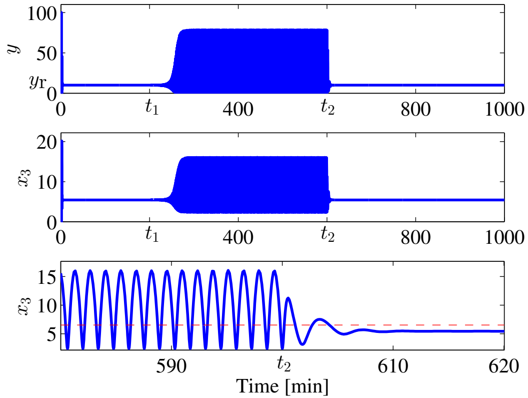

Figure: Time-domain behavior of x_3 and output y. The red dashed line indicates $1.2\,x_3^*$, with x_3^* as the steady state value of the state variable x_3 for $t > t_2$.

Estimation algorithms

The model

$$x_{t+1} = \begin{bmatrix} \Phi(\alpha_t) & 0_{3\times 2} \\ 0_{2\times 3} & I \end{bmatrix} \begin{bmatrix} \overline{x}_t \\ \alpha_t \\ \gamma_t \end{bmatrix} + \begin{bmatrix} \Gamma(\alpha_t) \\ 0_{2\times 1} \end{bmatrix} u_t + v_t$$

$$\equiv f(x_t, u_t) + v_t\,,$$

$$y_t = \frac{100\, C_{50}^{\gamma_t}}{C_{50}^{\gamma_t} + (C\, x_t)^{\gamma_t}} + e_t \equiv h(x_t) + e_t\,,$$

alexander.medvedev@it.uu.se

UPPSALA UNIVERSITET

Estimation algorithms

The model

$$x_{t+1} = \begin{bmatrix} \Phi(\alpha_t) & 0_{3\times 2} \\ 0_{2\times 3} & I \end{bmatrix} \begin{bmatrix} \overline{x}_t \\ \alpha_t \\ \gamma_t \end{bmatrix} + \begin{bmatrix} \Gamma(\alpha_t) \\ 0_{2\times 1} \end{bmatrix} u_t + v_t$$

$$\equiv f(x_t, u_t) + v_t \,,$$

$$y_t = \frac{100\, C_{50}^{\gamma_t}}{C_{50}^{\gamma_t} + (C\, x_t)^{\gamma_t}} + e_t \equiv h(x_t) + e_t \,,$$

State-of-the-art nonlinear recursive estimation algorithms:

- Extended Kalman Filter (EKF)

alexander.medvedev@it.uu.se

Estimation algorithms

The model

$$x_{t+1} = \begin{bmatrix} \Phi(\alpha_t) & 0_{3\times 2} \\ 0_{2\times 3} & I \end{bmatrix} \begin{bmatrix} \overline{x}_t \\ \alpha_t \\ \gamma_t \end{bmatrix} + \begin{bmatrix} \Gamma(\alpha_t) \\ 0_{2\times 1} \end{bmatrix} u_t + v_t$$

$$\equiv f(x_t, u_t) + v_t\,,$$

$$y_t = \frac{100\, C_{50}^{\gamma_t}}{C_{50}^{\gamma_t} + (C\, x_t)^{\gamma_t}} + e_t \equiv h(x_t) + e_t\,,$$

State-of-the-art nonlinear recursive estimation algorithms:

- Extended Kalman Filter (EKF)
- Particle Filter (PF)

alexander.medvedev@it.uu.se

Estimation algorithms

The model

$$x_{t+1} = \begin{bmatrix} \Phi(\alpha_t) & 0_{3\times 2} \\ 0_{2\times 3} & I \end{bmatrix} \begin{bmatrix} \overline{x}_t \\ \alpha_t \\ \gamma_t \end{bmatrix} + \begin{bmatrix} \Gamma(\alpha_t) \\ 0_{2\times 1} \end{bmatrix} u_t + v_t$$

$$\equiv f(x_t, u_t) + v_t \,,$$

$$y_t = \frac{100\, C_{50}^{\gamma_t}}{C_{50}^{\gamma_t} + (C\, x_t)^{\gamma_t}} + e_t \equiv h(x_t) + e_t \,,$$

State-of-the-art nonlinear recursive estimation algorithms:

- Extended Kalman Filter (EKF)
- Particle Filter (PF)
    - Sampling importance resampling (SIR PF)

alexander.medvedev@it.uu.se

Estimation algorithms

The model

$$x_{t+1} = \begin{bmatrix} \Phi(\alpha_t) & 0_{3\times 2} \\ 0_{2\times 3} & I \end{bmatrix} \begin{bmatrix} \overline{x}_t \\ \alpha_t \\ \gamma_t \end{bmatrix} + \begin{bmatrix} \Gamma(\alpha_t) \\ 0_{2\times 1} \end{bmatrix} u_t + v_t$$
$$\equiv f(x_t, u_t) + v_t\,,$$

$$y_t = \frac{100\, C_{50}^{\gamma_t}}{C_{50}^{\gamma_t} + (C\, x_t)^{\gamma_t}} + e_t \equiv h(x_t) + e_t\,,$$

State-of-the-art nonlinear recursive estimation algorithms:

- Extended Kalman Filter (EKF)
- Particle Filter (PF)
  - Sampling importance resampling (SIR PF)
  - Orthogonal basis particle filter (OBPF)

alexander.medvedev@it.uu.se

Estimation algorithm: EKF

The nonlinear model is used with state updates calculated from linearized dynamics

$$
\begin{aligned}
H_t &= \left.\frac{\partial h(x)}{\partial x}\right|_{x=\hat{x}_{t|t-1}} \\
K_t &= P_{t|t-1} H_t^T [H_t P_{t|t-1} H_t^T + R]^{-1} \\
\hat{x}_{t|t} &= \hat{x}_{t|t-1} + K_t [y_t - h(\hat{x}_{t|t-1})] \\
P_{t|t} &= P_{t|t-1} - K_t H_t P_{t|t-1} \\
\hat{x}_{t+1|t} &= f(\hat{x}_{t|t}, u_t) \\
F_t &= \left.\frac{\partial f(x, u_t)}{\partial x}\right|_{x=\hat{x}_{t|t}} \\
P_{t+1|t} &= F_t P_{t|t} F_t^T + Q\,.
\end{aligned}
$$

Estimation algorithm: PF

Sampling importance resampling (SIR) PF:

- $x^{(i)}$ denote a particle, $i = 1, 2, \ldots, N$
- $w^{(i)}$ the corresponding weight
- N the number of particles
- $v_t^{(i)}$ is a draw from $p_v(v)$, the process noise distribution
- $p_e(e)$ is the measurement noise distribution

$$
\begin{aligned}
\tilde{x}_{t+1}^{(i)} &= f(x_t^{(i)}, u_t) + v_t^{(i)} \\
\tilde{w}_{t+1}^{(i)} &= w_t^{(i)} p_e(y_t - h(\tilde{x}_t^{(i)}, u_t)) \\
w_{t+1}^{(i)} &= \tilde{w}_{t+1}^{(i)} / \sum_{j=1}^{N} \tilde{w}_{t+1}^{(j)} \\
\hat{x}_{t+1} &= \sum_{j=1}^{N} w_{t+1}^{(j)} x_{t+1}^{(j)} .
\end{aligned}
$$

alexander.medvedev@it.uu.se

Estimation algorithm: OBPF

- The OBPF follows the steps of the PF
- An orthogonal series is fitted to the particle set in the resampling step

$$p(x_t|Y_t) \approx \sum_{\mathbf{k}\in\mathbf{K}} a_t^{(\mathbf{k})} \phi_{\mathbf{k}}(x_t)\,,$$

  where $a_t^{(\mathbf{k})}$ is the coefficient for the basis function $\mathbf{k}$.
- The Hermitian basis functions are used. In the one-dimensional case

$$\phi_0(x) = \pi^{-1/4} \mathrm{e}^{-x^2/2},\ \phi_1(x) = \sqrt{2} x \phi_0(x)\,,$$
$$\phi_k(x) = \sqrt{\frac{2}{k}} x \phi_{k-1}(x) - \sqrt{\frac{k-1}{k}} \phi_{k-2}(x)\,.$$

alexander.medvedev@it.uu.se

Estimation algorithm: OBPF

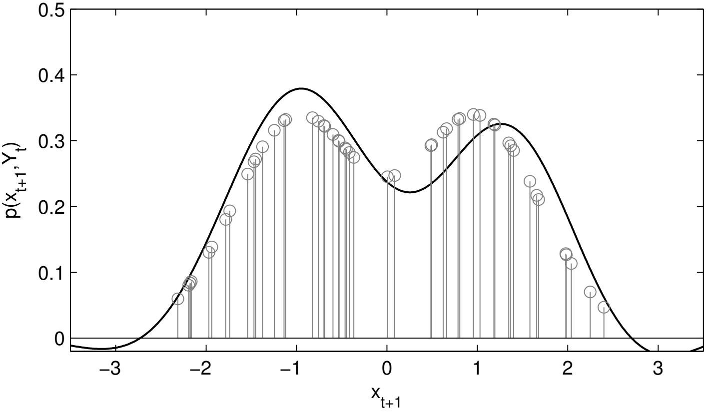

Figure: A set of **50** weighted particles (gray stems) and the fitted series expansion (black solid line) using the first **7** Hermite functions.

alexander.medvedev@it.uu.se

Estimation algorithm: OBPF

- The OBPF is developed for efficient computations on parallel platforms
- The global information on the estimated quantity expressed by the particles is compressed to a few expansion coefficients
- The OBPF exhibits higher parallelizability and estimation accuracy of compared to the SIR PF and the Gaussian PF

alexander.medvedev@it.uu.se

Estimation algorithm: OBPF

- The OBPF is developed for efficient computations on parallel platforms
- The global information on the estimated quantity expressed by the particles is compressed to a few expansion coefficients
- The OBPF exhibits higher parallelizability and estimation accuracy of compared to the SIR PF and the Gaussian PF

O. Rosén, A. Medvedev "Parallel Recursive Estimation Using Monte Carlo and Orthogonal Series Expansions", American Control Conference, Chicago, USA, July 2015.

alexander.medvedev@it.uu.se

Experiments

The EKF, the SIR PF, and the OBPF have been evaluated on

- Synthetic data: 48 synthetic data sets generated from real cases
- Clinical data: 48 data sets collected during PID-controlled administration of atracurium under general anesthesia

alexander.medvedev@it.uu.se

Experiments

The EKF, the SIR PF, and the OBPF have been evaluated on

- Synthetic data: 48 synthetic data sets generated from real cases
- Clinical data: 48 data sets collected during PID-controlled administration of atracurium under general anesthesia

Anesthesia phases:

1. $0 < t \leq 10$ min, induction (initial bolus), open loop

alexander.medvedev@it.uu.se

Experiments

The EKF, the SIR PF, and the OBPF have been evaluated on

- Synthetic data: 48 synthetic data sets generated from real cases
- Clinical data: 48 data sets collected during PID-controlled administration of atracurium under general anesthesia

Anesthesia phases:

1. $0 < t \leq 10$ min, induction (initial bolus), open loop
2. $10 < t \leq 30$ min, P-controller

alexander.medvedev@it.uu.se

UPPSALA UNIVERSITET

Experiments

The EKF, the SIR PF, and the OBPF have been evaluated on

- Synthetic data: 48 synthetic data sets generated from real cases
- Clinical data: 48 data sets collected during PID-controlled administration of atracurium under general anesthesia

Anesthesia phases:

1. $0 < t \leq 10$ min, induction (initial bolus), open loop
2. $10 < t \leq 30$ min, P-controller
3. $30 < t \leq 75$ min, from the beginning of the recovery from the initial bolus until the reference reaches its final value of 10%, PID-controller

alexander.medvedev@it.uu.se

Experiments

The EKF, the SIR PF, and the OBPF have been evaluated on

- Synthetic data: 48 synthetic data sets generated from real cases
- Clinical data: 48 data sets collected during PID-controlled administration of atracurium under general anesthesia

Anesthesia phases:

1. $0 < t \leq 10$ min, induction (initial bolus), open loop
2. $10 < t \leq 30$ min, P-controller
3. $30 < t \leq 75$ min, from the beginning of the recovery from the initial bolus until the reference reaches its final value of 10%, PID-controller
4. $75 < t \leq$ end, steady state, PID-controller

alexander.medvedev@it.uu.se

Experiments

The EKF, the SIR PF, and the OBPF have been evaluated on

- Synthetic data: 48 synthetic data sets generated from real cases
- Clinical data: 48 data sets collected during PID-controlled administration of atracurium under general anesthesia

Anesthesia phases:

1. $0 < t \leq 10$ min, induction (initial bolus), open loop
2. $10 < t \leq 30$ min, P-controller
3. $30 < t \leq 75$ min, from the beginning of the recovery from the initial bolus until the reference reaches its final value of 10%, PID-controller
4. $75 < t \leq$ end, steady state, PID-controller

alexander.medvedev@it.uu.se

Experiments

The EKF, the SIR PF, and the OBPF have been evaluated on

- Synthetic data: 48 synthetic data sets generated from real cases
- Clinical data: 48 data sets collected during PID-controlled administration of atracurium under general anesthesia

Anesthesia phases:

1. $0 < t \leq 10$ min, induction (initial bolus), open loop
2. $10 < t \leq 30$ min, P-controller
3. $30 < t \leq 75$ min, from the beginning of the recovery from the initial bolus until the reference reaches its final value of 10%, PID-controller
4. $75 < t \leq$ end, steady state, PID-controller

Rocha, C., Mendonca, T., and Silva, M.E. (2013). Modelling neuromuscular blockade: a stochastic approach based on clinical data. Mathematical and Computer Modelling of Dynamical Systems, 19(6), 540–556.

Experiments: synthetic data

Case # 7

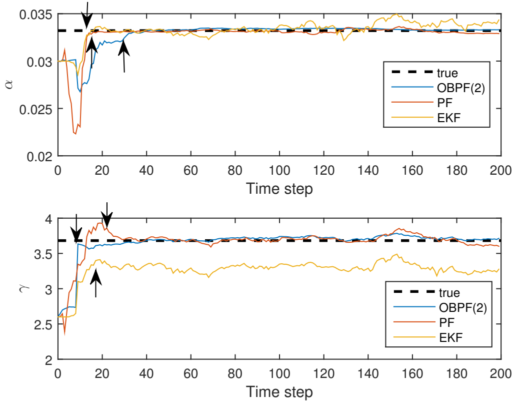

Figure: Estimated α (upper plot) and γ (bottom plot) for the Orthogonal Basis PF (OBPF), Sampling Importance Resampling PF and EKF for case number 7 in the synthetic database. The settling time instants are marked by the arrows.

Experiments: synthetic data

Bias

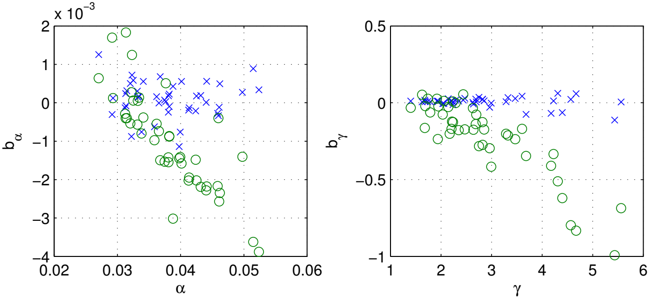

Figure: The true α and γ vs. estimation bias b_α and b_γ, respectively, for the 48 cases in the synthetic database. EKF – green circles, PF – blue crosses.

Rosén, Silva, Medvedev, Nonlinear Estimation of a Parsimonious Wiener Model for the Neuromuscular Blockade in Closed-loop Anesthesia, *IFAC World Congress*, Cape Town, South Africa, August, 2014.

Experiments: synthetic data

RMSE

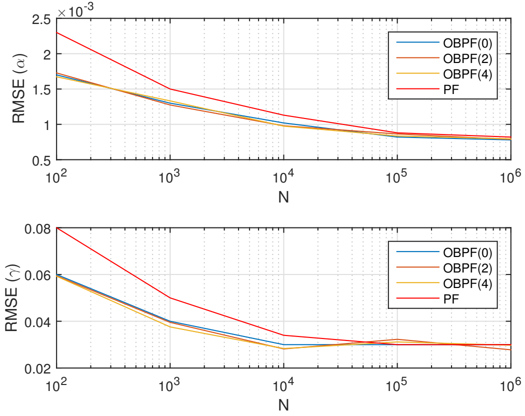

Figure: Root mean square error $R = \sqrt{\frac{1}{T}\sum_{t=0}^{T}(x_t - \hat{x}_t)^2}$ for α (upper plot) and γ (lower plot) as a function of the number of particles N.

alexander.medvedev@it.uu.se

Experiments: synthetic data

PDF estimation by PBPF

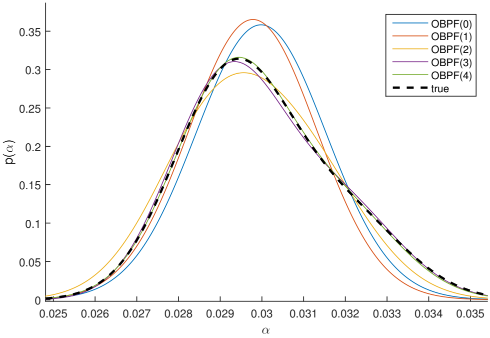

Figure: Marginal distribution for α at time $t = 5$min. The true PDF is shown in dashed black line. The approximations obtained by the OBPF with approximation orders from 0 to 4 are shown in colored solid lines.

Experiments: clinical data

Case # 39

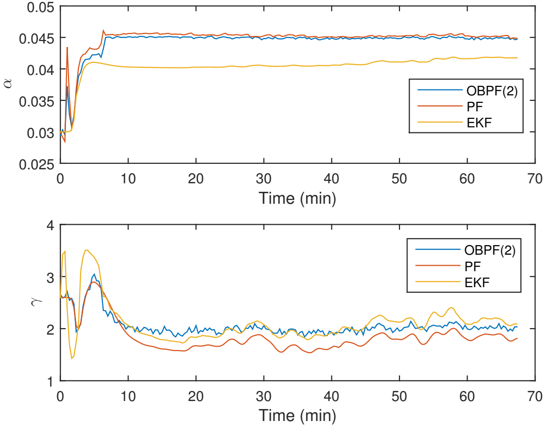

Figure: Estimated model parameters for the EKF, in dashed green, and the PF, in solid blue, over time for a case number 39 in the real database.

Experiments: clinical data

Output error

Table: Output error (absolute value) of estimation for the EKF, the PF and the OBPF, during the four phases of anesthesia; Best, Worst.

	EKF			PF		
Phase	mean	stdv	[min,max]	mean	stdv	[min,max]
1	**4.16**	0.62	[2.58,5.42]	0.95	0.47	[0.24,2.34]
2	0.49	0.17	[0.16,0.85]	0.58	0.39	[0.14,1.97]
3	0.31	0.16	[0.08,0.98]	0.30	0.16	[0.13,0.77]
4	0.25	0.16	[0.04,0.97]	0.25	0.13	[0.07 0.76]
	OBPF(0)			OBPF(5)		
Phase	mean	stdv	[min,max]	mean	stdv	[min,max]
1	**0.87**	0.53	[0.32,1.98]	0.90	0.44	[0.18,2.14]
2	0.52	0.15	[0.15,1.22]	0.52	0.18	[0.17,1.52]
3	0.31	0.18	[0.06,0.85]	0.28	0.18	[0.05,0.74]
4	0.26	0.16	[0.04,0.78]	0.23	0.14	[0.05 0.69]

Computational complexity of PF

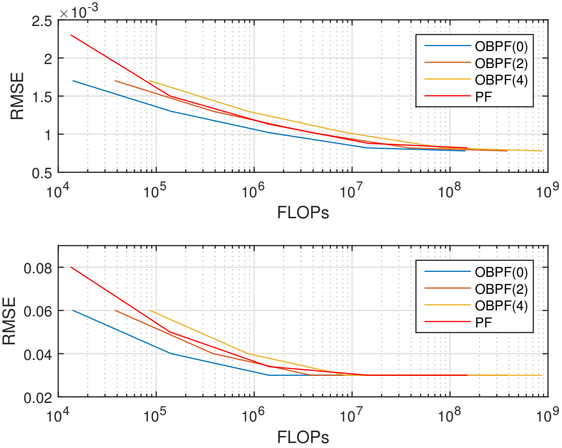

Figure: RMSE as a function of the number of floating-point operations per second (FLOPS) required for filter execution.

Conclusions

- A PID-tuning policy to automatically recover from undesired nonlinear oscillations in a drug delivery system is proposed

alexander.medvedev@it.uu.se

UPPSALA UNIVERSITET

Conclusions

- A PID-tuning policy to automatically recover from undesired nonlinear oscillations in a drug delivery system is proposed
- A time-varying proportional PID gain is shown to preserve the type of equilibria as in the case of constant controller gains.

alexander.medvedev@it.uu.se

Conclusions

- A PID-tuning policy to automatically recover from undesired nonlinear oscillations in a drug delivery system is proposed
- A time-varying proportional PID gain is shown to preserve the type of equilibria as in the case of constant controller gains.
- The recovery from oscillation time after applying the proposed time-varying PID gain is evaluated in simulation for a database of 48 cases, with the average recovery time of 4.22 min.

alexander.medvedev@it.uu.se

Conclusions

- A PID-tuning policy to automatically recover from undesired nonlinear oscillations in a drug delivery system is proposed
- A time-varying proportional PID gain is shown to preserve the type of equilibria as in the case of constant controller gains.
- The recovery from oscillation time after applying the proposed time-varying PID gain is evaluated in simulation for a database of 48 cases, with the average recovery time of 4.22 min.
- Use a particle filter to estimate a Wiener model when there is a large variation of the system variables, as in the induction phase of anesthesia.

alexander.medvedev@it.uu.se

Conclusions

- A PID-tuning policy to automatically recover from undesired nonlinear oscillations in a drug delivery system is proposed
- A time-varying proportional PID gain is shown to preserve the type of equilibria as in the case of constant controller gains.
- The recovery from oscillation time after applying the proposed time-varying PID gain is evaluated in simulation for a database of 48 cases, with the average recovery time of 4.22 min.
- Use a particle filter to estimate a Wiener model when there is a large variation of the system variables, as in the induction phase of anesthesia.
- Extended Kalman Filter is sufficient for tracking the model parameters around a set point, as in the maintenance phase of anesthesia.

Conclusions

- A PID-tuning policy to automatically recover from undesired nonlinear oscillations in a drug delivery system is proposed
- A time-varying proportional PID gain is shown to preserve the type of equilibria as in the case of constant controller gains.
- The recovery from oscillation time after applying the proposed time-varying PID gain is evaluated in simulation for a database of 48 cases, with the average recovery time of 4.22 min.
- Use a particle filter to estimate a Wiener model when there is a large variation of the system variables, as in the induction phase of anesthesia.
- Extended Kalman Filter is sufficient for tracking the model parameters around a set point, as in the maintenance phase of anesthesia.
- The Orthogonal Basis Particle FIlter offers the best computation/performance ratio.

alexander.medvedev@it.uu.se

PID controller tuning

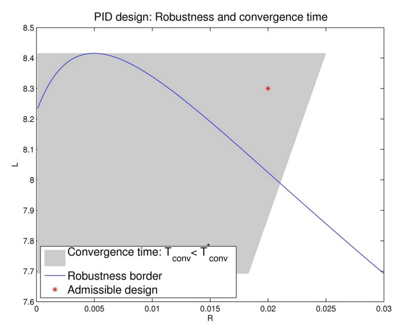

PID design procedure in terms of (R, L). The model parameters $\alpha = 0.027$, $\gamma = 2.4395$. Design specifications: $r^* = 40\%$, $T^*_{\text{conv}} = 30$ min.. The shaded area corresponds to the designs with $T_{\text{conv}} \leq T^*_{\text{conv}}$ The top side of the boundary $\chi(\alpha_{\min}, L, R) = 0$ (blue line) determines the region of controller robustness over $r^* = \frac{\alpha_{\min}}{\alpha}$. The red star depicts an admissible design $(L = 8.3, R = 0.02)$ with $r = 42.178\%$ and $T_{\text{conv}} = 26.8$ min.

alexander.medvedev@it.uu.se

UPPSALA UNIVERSITET

Manual administration in NMB

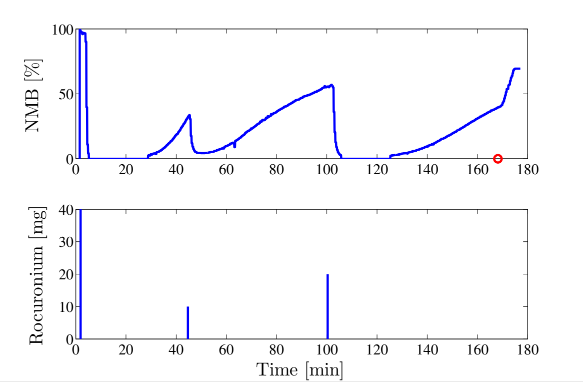

Manual administration rocuronium. Upper plot: First twitch of a TOF stimulation normalized by the reference twitch, quantifying the NMB level. Bottom plot: rocuronium bolus. o on marks the time when a bolus of atropine and neostigmine is intravenously administered to fasten the recovery from the NMB.

alexander.medvedev@it.uu.se